

The logo for EPJ B consists of a dark blue rectangle. The left side of the rectangle is a vertical strip with a textured, orange-red pattern. The letters 'EPJ B' are written in a white, serif font across the blue background.

*EPJ B*

[www.epj.org](http://www.epj.org)

Condensed Matter  
and Complex Systems

Eur. Phys. J. B **63**, 239–243 (2008)

DOI: 10.1140/epjb/e2008-00238-2

## Metastability and functional integration in anisotropically coupled map lattices

A. Pitti, M. Lungarella and Y. Kuniyoshi



# Metastability and functional integration in anisotropically coupled map lattices

A. Pitti<sup>1,a</sup>, M. Lungarella<sup>1,2</sup>, and Y. Kuniyoshi<sup>1,3</sup>

<sup>1</sup> ERATO Synergistic Intelligence Project, JST, The University of Tokyo, 113-8656 Tokyo, Japan

<sup>2</sup> Artificial Intelligence Lab, University of Zurich, 8050 Zurich, Switzerland

<sup>3</sup> ISI Laboratory, Dept. of Mechano-Informatics, The University of Tokyo, 113-8656 Tokyo, Japan

Received 6 February 2008 / Received in final form 28 April 2008

Published online 20 June 2008 – © EDP Sciences, Società Italiana di Fisica, Springer-Verlag 2008

**Abstract.** Metastability is a property of systems composed of many interacting parts wherein the parts exhibit simultaneously a tendency to function autonomously (local segregation) and a tendency to cooperate (global integration). We study anisotropically coupled map lattices and discover that for specific values of the coupling control parameters the entire system transits to a metastable regime. We show that this regime manifests a quasi-stable state in which the system can flexibly switch to another such state. We briefly discuss the relevance of our findings for information processing, functional integration, metastability in the brain, and phase transitions in complex systems.

**PACS.** 05.45.Ra Coupled map lattices – 64.60.My Metastable phases

In recent years, much attention has been paid to collective behavior in networks of dynamical systems [1,2]. A large number of studies have identified different kinds of synchronization in a broad class of natural and artificial systems (e.g., fireflies, cells, and atoms; see [3] and references therein). Particular attention has been devoted to the degree of collective organization measured as the tendency of separately operating (functionally segregated) subsystems of a network to exhibit coherent (functionally integrated) dynamics. Important examples are neural assemblies which are spatially separated cortical subsystems composed of thousands of neurons exhibiting multiple time scale dynamics [4–7]. It is natural to ask what qualitative features (control parameters) enable emergence of global integration and local segregation in systems with many degrees of freedom (e.g., [8–12]). Moreover, one might wonder how the individual dynamical processes composing the whole perform their unique roles expressing their own form of information, while at the same time being functionally connected and constrained by the interactions with other processes. Such interplay between functional local autonomy and coordinated global activity is a distinguishing trait of metastability [13–15]. In such regime, the entire system is in a state of optimal flexibility and can rapidly shift from one attractor to another (e.g., [13]).

In this paper, we focus our attention on the relation between metastability and functional integration. Particularly, we investigate the conditions for such a metastable regime to emerge in diffusively coupled map lattices of logistic maps. We extend the coupled map lattices model (CML) [16] and consider a multi-lattice system in which each chaotic unit is also coupled to units of other lattices (see [17], for a similar extension) as it is the case in sparse networks. We discover that the values of the coupling strength of units to the network (diffusing coefficient or total coupling) and the coupling strength between units belonging to the same lattice and to other lattices (intra- and inter-lattice coupling ratio) significantly influence the occurrence of global integration and local segregation. For specific combinations of the two coupling parameters, units belonging to different lattices mutually lock their phases while they continue to operate as specialized, autonomous entities. The global integrative tendency displayed by the entire system is characterized by temporal correlations between spatially remote (not directly coupled) units. Moreover, each unit transits to a bistable state becoming at the same time member of two or more lattices and acquiring “novel” information processing capabilities, where the information is encoded in the phase delays between the units.

Let  $f$  be the map that governs the dynamics of each chaotic unit, and let  $x_n^k(i, j)$  represent the activity of the unit at lattice site  $(i, j)$  of the  $k$ th lattice at discrete time step  $n$ . Additionally, let  $F_n^k(i, j)$  be the diffusive coupling

<sup>a</sup> e-mail: alex@isi.imi.i.u-tokyo.ac.jp

term between units located on lattice  $k$  (von Neumann neighborhood of order 1):

$$F_n^k(i, j) = \frac{x_n^k(i-1, j) + x_n^k(i+1, j) + x_n^k(i, j-1) + x_n^k(i, j+1)}{4} \quad (1)$$

and let  $G_n^k(i, j)$  be the coupling term between units located on lattices  $k-1$  and  $k+1$  (Laplace neighborhood):

$$G_n^k(i, j) = \frac{x_n^{k-1}(i, j) + x_n^{k+1}(i, j)}{2}. \quad (2)$$

For both coupling directions, we assume periodic boundary conditions. The dynamics of unit  $(i, j)$  of lattice  $k$  at time  $n+1$  is described by the following equation:

$$x_{n+1}^k(i, j) = (1 - \gamma) f_\alpha(x_n^k(i, j)) + \gamma \epsilon F_n^k(i, j) + \gamma(1 - \epsilon) G_n^k(i, j) \quad (3)$$

where  $\epsilon \in [0, 1]$  is the relative intra- and inter-lattice coupling ratio of individual units among and between the lattices and  $\gamma \in [0, 1]$  is the coupling strength to the network. The multi-lattice system consists of  $K$  lattices ( $k = 1, \dots, K$ ) composed each of  $L \times L$  chaotic units. The local dynamics is governed by the logistic map  $f_\alpha(u) = 1 - \alpha u^2$  which is chosen due to its rich dynamical structure controlled by a single parameter  $\alpha \in [0.0, 2.0]$ . For all numerical experiments, we consider  $K = 4$  maps with  $L = 100$  units, and fix  $\alpha$  to 2.0 for which the logistic map is at its most entropic regime. Unless otherwise specified, numerical simulations are started with random initial conditions and last for 1000 iterations.

Our aim is to understand the relationship between the functional characteristics of the multi-lattice responsible for information processing and the structural characteristics of the underlying network. We take the stance of complex networks and analyze global integration of functionally segregated groups of chaotic units. Integration is defined as the multivariate generalization of mutual information and captures the system's overall deviation from statistical independence [18–20]. It captures the total amount of statistical dependency among a set of random variables  $X_i$  forming elements of a system  $X = \{x_i\}$ . Integration is defined as the difference between the individual entropies of the elements and their joint entropy [19]. In the case of the lattice, integration is the difference between the sum of entropies of the activity of the chaotic units  $\{x_n^k(i, j)\}$  and the entropy of the system considered as a whole,  $X = \{x_n^k(1, 1), x_n^k(1, 2), \dots\}$ . While the individual entropies are easily estimated through the single-point probability  $p_{i,j}(z)$  that  $x_n^k(i, j)$  takes value  $z$ , the evaluation of the entropy  $H(Z)$  of the entire lattice is nontrivial because it requires a number of samples which grows exponentially in the size  $L$  of the lattice.

We use formulae derived in [19,21] and estimate the integration  $I(X)$  by first resampling the original time series to yield Gaussian signal amplitudes  $X_g$  and then using the

correlation matrix  $COR(X_g)$ :

$$I(X) = \sum_{i=1}^n H(\{x_i\}) - H(X) \approx -\frac{\ln(|COR(X_g)|)}{2} \quad (4)$$

where the correlation coefficient  $COR(X_g(A), X_g(B))$  between two random variables  $A$  and  $B$  with mean values  $\mu_{X_g(A)}$  and  $\mu_{X_g(B)}$  and standard deviations  $\sigma_{X_g(A)}$  and  $\sigma_{X_g(B)}$  is defined as

$$COR(X_g(A), X_g(B)) = \frac{E((X_g(A) - \mu_{X_g(A)})(X_g(B) - \mu_{X_g(B)}))}{\sigma_{X_g(A)}\sigma_{X_g(B)}}.$$

In order to identify the modes of interaction that occur within one lattice and among lattices, we calculate the integration  $I_{intra-CML}$  in one arbitrarily chosen lattice (all lattices are identical) and the integration  $I_{inter-CML}$  between all lattices composing the multi-lattice (here, calculated considering the joint activity of four lattices). Figures 1a and 1b show  $I_{intra-CML}$  and  $I_{inter-CML}$  evaluated by varying the parameter  $\epsilon$ , the coupling ratio coefficient between intra- and inter-lattices, and  $\gamma$ , the coupling strength of the individual units to the network. For weak couplings  $\gamma < 0.15$ , but regardless of  $\epsilon$ ,  $I_{intra-CML} \approx 0$  and  $I_{inter-CML} \approx 0$ , and the chaotic units are essentially independent. For  $0.15 < \gamma < 0.45$ , the entire system can undergo phase transitions. Specifically, the transitions occur for combinations of couplings such that  $6 < I_{intra-CML} < 10$  and  $6 < I_{inter-CML} < 10$  (dashed box in Fig. 1c). In the new regime, the chaotic units are susceptible to cooperate with units of neighboring lattices as well as with “in-lattice” neighbors (as we will demonstrate with additional analysis below; see the snapshots of the maps in Fig. 2). By further increasing  $\gamma$ , the ratio between in-map activity and external activity switch from multi-lattice integration for  $\epsilon < 0.45$  in Figure 1b to in-lattice integration (transition roughly for  $\epsilon > 0.45$ , Fig. 1a). An interesting result is that global integration is sensitive to the network organization parameter  $\epsilon$  rather than the behaviour of the individual units (coupling  $\gamma$ ). That is, a global property such as  $I_{inter-CML}$  is strongly influenced by the system's organization controlled by parameter  $\epsilon$ . A state from which the system is able to reach its mesoscopic scale — the scale at which the properties of the system become independent from the behavior of the individual units composing it, but depends only on the network's global structure.

To better understand how integration affects the interaction between the lattices, we analyze the coordination relation of a set of units with their in-lattice neighbors and compare it with the coordination relation with units of neighboring lattices. The two measured collective variables are (1) the averaged phase difference  $\Delta\phi_{intra-CML}$  over the phase of one arbitrarily chosen unit  $x_n^k(i, j)$  and the phase of its four neighbors [e.g.,  $x_n^k(i \pm 1, j \pm 1)$ ], and (2) the averaged phase difference  $\Delta\phi_{inter-CML}$  between  $x_n^k(i, j)$  and the two units of the neighboring lattices [e.g.,  $x_n^{k \pm 1}(i, j)$ ]; where the time averages are calculated over

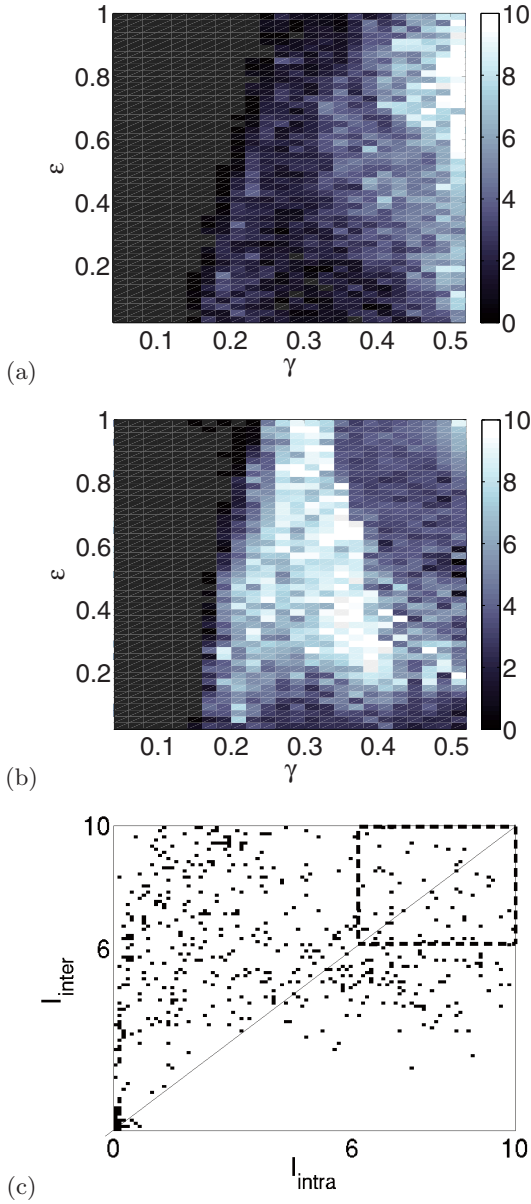


**Fig. 1.** Integration as a function of the intra/inter-lattice coupling ratio  $\epsilon$  and the coupling strength of the individuals to the network  $\gamma$ . The resolution is 0.02 in the interval  $[0, 1]$ . (a) Integration  $I_{intra-CML}$  within one lattice ( $L \times L$ ;  $L = 100$ ). (b) Integration  $I_{inter-CML}$  for the multi-lattice ( $4 \times L \times L$  units). (c) The dashed box indicates the interval of values of  $I_{intra-CML}$  and  $I_{inter-CML}$  for which the system is in a metastable regime.

10000 iterations. Figures 3a and 3b show the relative phase as a function of the parameter  $\gamma$ , for  $\gamma \in [0, 0.75]$  and  $\epsilon = 0.75$ .

As evident from Figure 3, the phase relationships for the units within the lattice and among units of distinct lattices display different profiles as a function of  $\gamma$ , confirming that “two” processes are actually involved (i.e., within the lattices and among them). For small values of the intra-lattice coupling (roughly for  $\gamma < 0.25$ ), the lo-



**Fig. 2.** Snapshot pattern of the multi-lattice for  $\{\gamma, \epsilon\} = \{0.42, 0.82\}$  at time step  $n = 1000$ . A gray-scale plot is adopted for each pixel according to  $x_n^k(i, j)$ . Clusters are dynamic and evolve over time, synchronizing and desynchronizing while exchanging information.

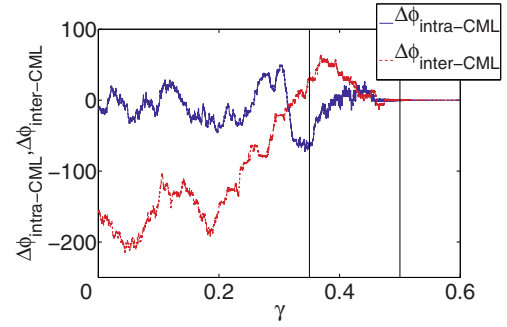


**Fig. 3.** Relative phase as a function of the coupling  $\gamma$  between “in-lattice” neighbors,  $\Delta\phi_{intra-CML}$  (average over 4 neighbors), and between “out-of-lattice” neighbors,  $\Delta\phi_{inter-CML}$  (average over 2 neighbors);  $\gamma \in [0, 0.6]$  and  $\epsilon = 0.75$ . For  $\gamma \in [0.37, 0.50]$ , the units of the four lattices tend to phase-lock with both “in-” and “out-of-lattice” neighbors simultaneously.

cal interactions between the units are weak, small fluctuations are damped and do not lead to any changes at the system’s scale. Spontaneous global phase synchronization occurs for  $0.37 < \gamma < 0.5$ . In this interval, fluctuations are amplified, the maps exhibit global stabilization, and the phase difference  $\Delta\phi$  with neighbors ( $d(\Delta\phi)/d\gamma \approx 0$ ; Figs. 3a and 3b). The individual units transit to a bistable state and become members of the cluster formed by local neighbors as well as members of the cluster formed with “distant” units. Interestingly, the activities of the individual units in each CML co-located at the same position  $x_n(i, j)$  differentiate and their dynamics exhibit two distinct rhythms (indicating their biphasic nature) (Figs. 4a to 4d). The entire system bifurcates to a metastable regime acquiring structure at several level of organizations.

When the chaotic maps synchronize, they exchange energy through their phase dynamics. In this particular biphasic state, it is of some interest to study its capability to process information acquired through an external input. To do so, we modify the equation governing the local dynamics of the lattice at site  $(i, j)$  by coupling it to an external input  $s_n(i, j)$ . By including this new information source, the equation of the inter-lattice coupling term

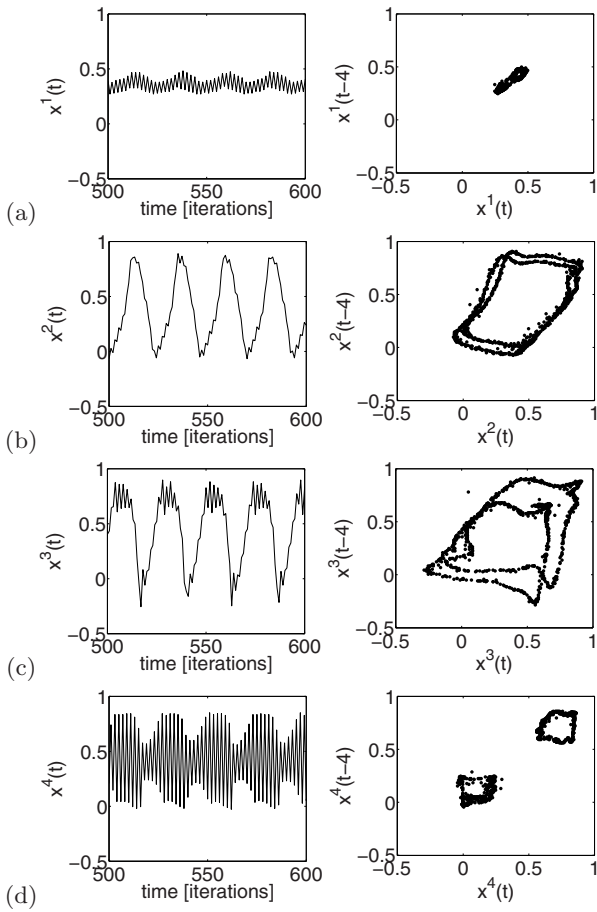


**Fig. 4.** Metastability. Time series (left) and phase plots (right) of four chaotic units located at the same coordinates (arbitrarily chosen) in one of the four coupled lattices for  $\{\gamma, \epsilon\} = \{0.40, 0.75\}$ . The four units are in-phase and exhibit bistability as demonstrated by the presence of two limit-cycle attractors. They present distinct but coordinated dynamics.

(Eq. (2)) for map  $k = 1$  becomes:

$$G_n^1(i, j) = \frac{x_n^4(i, j) + x_n^2(i, j)}{4} + \frac{s_n(i, j)}{2}. \quad (5)$$

An adequate way of estimating the qualitative aspects of the metastable system (e.g., its plasticity) is to measure its response to a step input. We apply a perturbation to the system for the parameter combination  $\{\gamma, \epsilon\} = \{0.42, 0.92\}$  for which the units are sensitive to even weak phase variations of coupled external signals. At non-specific time instants, we perturb a row of ten units of lattice  $k = 1$  by applying a unit step function  $s_\tau(i, j) = 1_\tau$  for a duration of  $\tau$  steps. We hypothesize that because the multi-lattice is in a “quasi-stable” state of dynamic balance, it can flexibly switch to another such state. That this is indeed the case is shown in Figure 5.

For instance, when the step signal  $s_\tau = 1$  perturbs the units dynamics at  $t = 180$ , the individual units deviate from their original trajectories and rapidly bifurcate

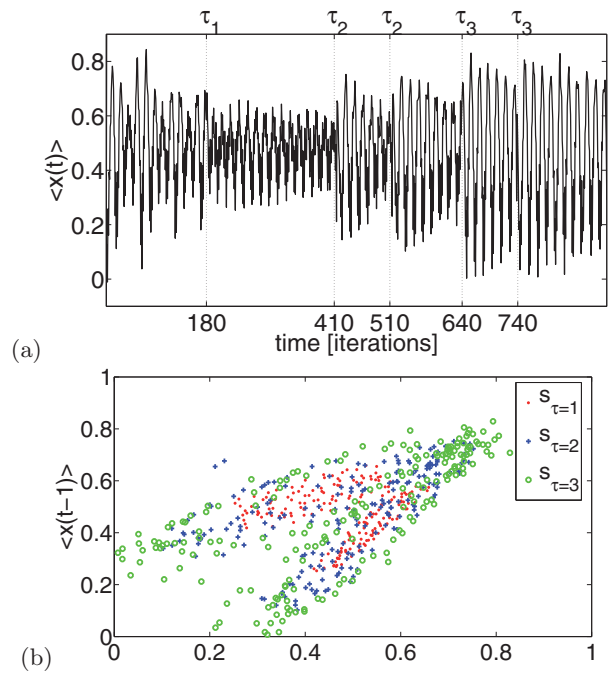


**Fig. 5.** Perturbation analysis. (a) Units mean response to a step function for different duration of  $\tau = 1$ ,  $\tau = 2$ , and  $\tau = 3$  time steps. (b) (Color online) Phase plot of the average group response for the three cases. Each point in the figure corresponds to the average over 10 units.

to a new metastable coordination relation (Fig. 5). Similar transitions occur for the step durations  $\tau = 2$  and  $\tau = 3$  (Fig. 5b shows the average group phase plot evolution for the three different perturbation cases). The perturbations applied to a small number of logistic maps affect the phase of the units belonging to the same group within the same lattice and all units start following the same rhythm. This result demonstrates that while being stable the entire system exhibits also plasticity being sensitive to external events with high temporal precision: an important characteristic of complex adaptive systems and dissipative structures [14].

In conclusion, we showed that specific local rules of interaction in chaotic maps can lead to an abrupt and spontaneous phase transition of the entire system. The anisotropy imposed on the couplings between the individual dynamical units leads to the coexistence of multiple dynamic regimes (e.g., two-phase mixtures), a property observed in many nonlinear phenomena (e.g., liquid-gas phase mixtures, nonlinear optics, or in nonequilibrium thermodynamics). This particularity enables the units to exchange information through their phases and to adapt to changing external constraints. External signals perturb the coordination between the units and modify their phase relations. As a result, information can be encoded as a phase delay between the units as it is done in phase-locked loop networks [22]. Hence, the system’s behavior evolves through the complex interplay of function, structure, and fluctuations — a characteristic of dissipative systems. In

neurobiology, this relates to the hypothesis that metastability and functional integration within and among specialized areas of the brain is mediated by effective connectivity [23]. A region of the brain is not perfectly delineated and may function autonomously for a moment, but strongly depend on input from other regions in the next moment, shifting between local activity and long-range coordination. This leads to a constant interplay between local and global synchrony exhibiting coherence and plasticity in neural activity. Such interplay between stability and plasticity is a necessary condition for adaptive behavior while maintaining an overall robustness in response to changing environment [14].

Plastic changes may be controlled through value systems capable of influencing the coupling between distinct maps in presence of changes in salient sensory stimulation, analogous to the neuromodulatory system [24]. More precisely, the global parameters pair  $\{\epsilon, \gamma\}$  play a role analogous to ascendant neuro-modulators, which favor or dismiss attentional blink or attentional access by modifying the connectivity and the functional property of the brain system. In our model, a global parameter can modify the geometry of the system and its functional connectivity when passing a critical threshold. Thus, it might be interesting for a system to work near this critical area in order to rapidly switch between computational capabilities or inhibitory mode. Hence in the brain, for a critical threshold, the ascending chemical neuromodulators are responsible for the synchronous activation of large neural ensembles producing multi-band frequencies oscillations [25]. Our results have to be compared with other studies investigating the dynamical organization in clustered neural networks (cf. [10–12]). These studies point out on the importance of network organization in a scale-free system showing efficiency for instance of small-world network class of complex systems to form plastic hierarchies. In our experiment, efficient organization of the network corresponds to high intra- and inter-maps integration. In future work, we will study whether these characteristics are related or not and whether they are encountered in other type of networks (e.g., spiking neural network [26]).

We would like to thank the JST ERATO project for the support to this research and the two anonymous reviewers for their valuable comments.

## References

1. R. Albert, A.L. Barabási, *Rev. Mod. Phys.* **74**, 47 (2002)
2. S. Boccaletti, V. Latora, Y. Moreno, M. Chavez, D. Hwang, *Phys. Rep.* **424**, 175 (2006)
3. A.S. Pikovsky, M.G. Rosenblum, J. Kurths, *Synchronization* (Cambridge Press, 2001)
4. J. Ito, K. Kaneko, *Phys. Rev. E* **67** (2003)
5. A. Venaille, P. Varona, M. Rabinovich, *Phys. Rev. E* **71**, (2005)
6. T. Pereira, M. Baptista, J. Kurths, *Eur. Phys. J. Special Topics* **146**, 155 (2007)
7. N. Masuda, K. Aihara, *Biological Cybernetics* **90**, (2004)
8. M. Ivancheko, G. Osipov, V. Shalfeev, J. Kurths, *Phys. Rev. Lett.* **93**, (2004)
9. G. Osipov, M. Ivancheko, J. Kurths, B. Hu, *Phys. Rev. E* **71** (2005)
10. C. Zhou, L. Zemanova, G. Zamora, C. Hilgetag, J. Kurths, *Phys. Rev. Lett.* **97**, (2006)
11. L. Zemanova, C. Zhou, J. Kurths, *Physica D* **224**, (2006)
12. C. Honey, R. Kotter, M. Breakspear, O. Sporns, *Proc. Natl. Acad. Sci. USA* **104**, 10240 (2007)
13. S.L. Bressler, J.A. Kelso, *Trends in Cognitive Science* **5**, 26 (2001)
14. A. Fingelkurts, A. Fingelkurts, *Int. J. Neurosc.* **114**, 843 (2004)
15. M.G. Werner, *Proceedings The Evolution of Human Cognition and Neuroscience* (Les Treilles, Provence, France, 2006)
16. K. Kaneko, *Prog. Theor. Phys.* **72**, 480 (1984)
17. Y. Dobyans, H. Atmanspacher, *Chaos, Solitons and Fractals* **28**, 755 (2006)
18. W. McGill, *IEEE Trans. Inform. Theory* **4**, 93 (1954)
19. G. Tononi, O. Sporns, G.M. Edelman, *Proc. Natl. Acad. Sci. USA* **91**, 5033 (1994)
20. E. Schneidman, S. Still, M.J. Berry, W. Bialek, *Phys. Rev. Lett.* **91**, 238701 (2003)
21. G. Tononi, O. Sporns, G.M. Edelman, *Proc. Natl. Acad. Sci. USA* **93**, 3422 (1996)
22. F.C. Hoppensteadt, E.M. Izhikevich, *Phys. Rev. E* **62**, 4010 (2000)
23. G. Tononi, O. Sporns, *BMC Neurosc.* **4**, 31 (2003)
24. K. Doya, *Neural Network* **15**, 495 (2002)
25. S. Dehaene, J. Changeux, *Plos* **3**, 1 (2005)
26. E. Izhikevich, G. Edelman, *PNAS* **105**, 3593 (2008)